

**FUNCTIONALISATION OF THE BOUNDARY LAYER BY DEFORMATION-INDUCED MARTENSITE ON BEARING RINGS BY MEANS OF BULK METAL FORMING PROCESSES**

Bernd-Arno BEHRENS, Kai BRUNOTTE, Hendrik WESTER, Julius PEDDINGHAUSEN,  
Michael TILL

*Leibniz University Hannover (LUH) - Institute of Forming Technology and Machines (IFUM), Garbsen,  
Germany, EU, [till@ifum.uni-hannover.de](mailto:till@ifum.uni-hannover.de)*

<https://doi.org/10.37904/metal.2022.4394>

**Abstract**

During cold forming of metastable austenitic steels, a strength-increasing phase transformation induced by externally superimposed stresses occurs in addition to strain hardening. The effect of deformation-induced martensite formation has so far not been utilized industrially in the area of bulk forming, but could be suitable for the production of highly-loaded components in oxidative atmospheres. The aim of this study is the analysis of local phase transformations in metastable austenitic steels in the boundary layer of bulk formed components. For this purpose, the relationship between the process conditions occurring during bulk metal forming and the resulting martensitic phase fraction was determined. Cylinder compression tests are carried out in which the influence of various process parameters can be investigated. These include forming temperature, true plastic strain and forming speed. In a quantitative measurement by means of a magnetic induction process, local martensite formation is determined and hardness measurements are carried out. The recorded flow stress curves are implemented in a numerical simulation. Furthermore, the influence of different tool surface topographies on the contact conditions of the workpiece-tool system is characterized by means of ring compression tests. With the numerical simulations and experimentally obtained results, a surface hardening process for bearing rings is designed. The relationship between local true plastic strain and deformation-induced martensite development is explained by material flow simulations, taking into account the process route for manufacturing the bearing ring and the varying friction factors.

**Keywords:** Bulk metal forming, phase transformation, local martensite formation

**1. INTRODUCTION AND MOTIVATION**

Bulk formed steel components are often subject to high mechanical and tribological loads [1]. In order to adapt their material properties, e.g. hardness, strength and ductility, they are heat-treated after forming. Stainless steels cannot be conventionally hardened and are seen unsuitable for high mechanical loads [2,3]. At room temperature, these steels are in an austenitic state with high formability [4]. During forming of metastable austenitic steels, the resulting strain hardening is significantly increased by an additional deformation-induced martensitic phase transformation. The phase transformation is accompanied by the introduction of compressive stresses due to the increase in volume of the martensitic phase, since the face-centred cubic (fcc) lattice prevailing in the initial state is more densely packed than the body centered cubic (bcc) lattice of the martensite [5]. In contrast to thermally induced hardening, this forming-induced hardening mechanism occurs when forming austenite below room-temperature. Numerous research papers have described the basic effects of phase transformation in metastable austenitic steels [6], however not with application in bulk forming. **Figure 1** shows the basic deformation-induced transformation process and the resulting solidification. The formed martensite consists of ferritic  $\alpha'$ -martensite, which has a tetragonal-distorted bcc lattice structure, and of unstable  $\epsilon$ -martensite with a hexagonal closest packed (hcp) structure. The lattice can transform into  $\alpha'$ -martensite under further stresses [7].

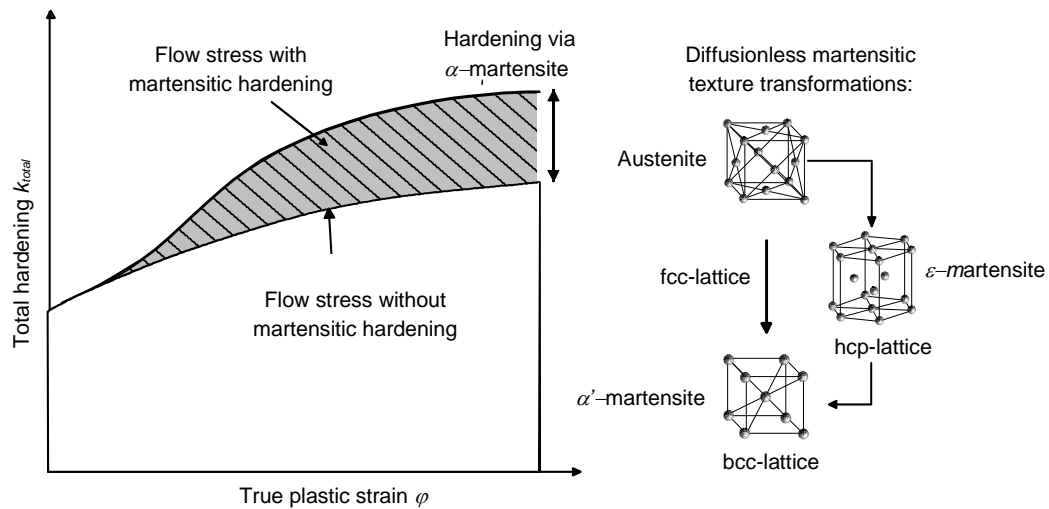


**Figure 1** Hardening of metastable austenitic materials [8]

The aim of this investigation is the local use of forming induced phase transformation in the surface layer of bulk components made of metastable austenitic steel X5CrNi18-10. The forming process is intended to specifically influence the material properties in the area near the surface and thus optimize the component properties especially the fatigue behavior of rolling contacts. For this purpose, the example of bulk formed angular contact ball bearing inner rings was investigated. To increase their service life, different tool surfaces and lubrication conditions are generated and investigated for their influence on the true plastic strain during forming.

## 2. MATERIALS AND METHODS

First, upsetting tests were carried out on forming simulators by Gleeble (type 3800-GTC) and Instron (plastometer, type DYN5J5590), to determine the influence of the forming parameters true plastic strain, forming temperature and speed as well as the resulting phase transformation on flow stress curves. The specimens ( $\varnothing 10$  mm x 15 mm; X5CrNi18) were tested at forming temperatures between  $T = -15$  and  $300$  °C and with constant strain rates of  $\dot{\varphi} = 0.1, 1$  and  $10$  s<sup>-1</sup>. The samples were upset in steps to the true plastic strains  $\varphi = 0.1, 0.3, 0.5$  and  $0.7$ . The temperatures at  $-15$  °C were achieved in a thermal forming container on the plastometer in order to keep the surrounding temperature constant. The specimens and the thermal container including the die were cooled down in a freezer to the forming temperature  $-15$  °C beforehand and monitored with thermocouples (type K). The tests with temperatures from  $20$  °C and above were carried out on the Gleeble forming simulator. Subsequently, the samples were investigated by means of magnetic inductive analysis (Feritscope MP3C) and hardness measurements (HV1) with regard to the deformation-induced martensitic phase transformation.

To determine the friction values with different surface treatments and varying lubricants and forming temperatures, ring upsetting tests were carried out full factorial on a Weingarten eccentric press type PSR 160 screw press. Various machining processes (grinding, blasting, turning) were used on the tool surface to investigate the contact conditions between the tool and workpiece surfaces and their influence on the deformation-induced martensitic phase transformation. In order to preserve the introduced surface topology of the tools, a duplex treatment (combination of nitriding and coating) of the surface layer was subsequently carried out. The manufacturing processes used enabled both direction-dependent and independent textures with varying texturing intensities. Three established lubricants for cold forging (molybdenum sulphide (MoS<sub>2</sub>), Teflon and CON TRAER G300) were investigated. The ring upsetting tests were also carried out at

temperatures of -15, 20, 150 and 300 °C in order to determine the thermal influence on the contact area. To determine the friction factors, the height and diameter differences of the upset rings were analyzed using corresponding nomograms. To keep the initial forming temperature constant and to achieve reproducible results, thermal containers were used during the forming process as well.

The aim of the subsequent material flow simulation was the quantification of the local true plastic strain in the formed component to determine optimal forming conditions. The surface hardening of the contact surfaces of inner angular contact ball bearing rings should thus be achieved by means of a forming process. With the determined material data and the friction factors, a 2D model was created in the commercial FE system simufact.forming 16.0. The semi-finished products were meshed with the element type quads (10) and the element size 0.2 mm. For the simulation a screw press with a gross energy of 40 kJ, a max. ram speed of 330 mm/s and an efficiency of 0.7 was predefined (analogous to the screw press used in the experiments). The final objective was to design a tooling system for the single-stage forming process which can be cooled with the sample and can be quickly installed and removed.

### 3. RESULTS AND DISCUSSION

**Figure 2** (left) illustrates the martensite content and the true plastic strain for X5CrNi18-10 at different forming temperatures in the upsetting tests. It shows that a significant increase in the martensite content is possible through additional cooling while forming. As a result of the forming process, an increase in the martensite content was observed. The martensitic phase content with a forming speed of  $\dot{\varphi} = 0.1 \text{ s}^{-1}$  and a temperature  $T = 20 \text{ °C}$  of 6.2 % was measured at the respective maximum true plastic strain of 0.7. Furthermore, the martensite content at the forming temperature -15 °C was around 22%. Therefore, the forming temperature has a significant influence on the deformation-induced martensitic phase transformation in X5CrNi18-10.

**Figure 2** (right) shows the influences of the forming speed on the deformation-induced martensitic phase transformation under increasing true plastic strain. With higher deformations (true plastic strain > 0.3), a dependence of the forming speed with regard to the martensite content can be determined. The decrease of the martensite content with higher forming speed can be attributed to the adiabatic heating during upsetting tests with high forming speed. The resulting higher temperature leads to a suppression of the martensite transformation during forming.

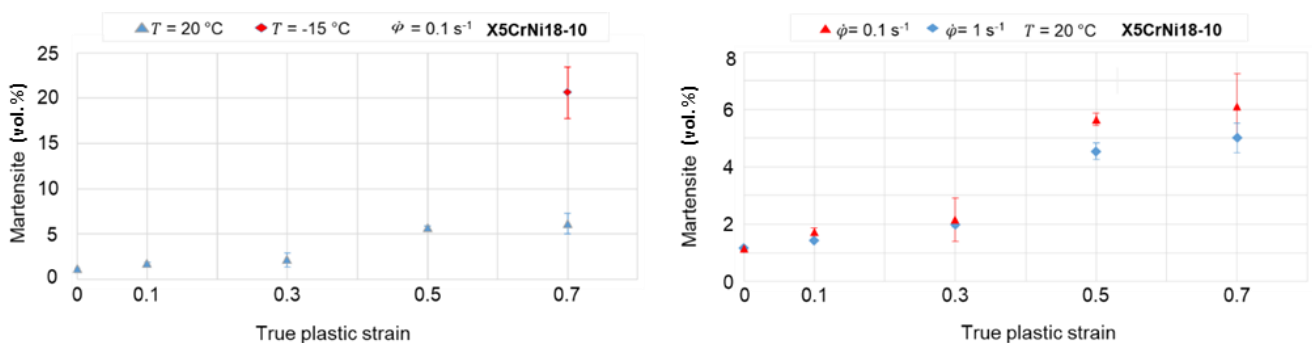


**Figure 2** Martensite content in upsetting samples (X5CrNi18-10) influenced by forming temperature (left) and forming speed (right)

Based on hardness values, deformation-induced martensitic phase transformation can be investigated as a function of true plastic strain, initial forming temperature and speed. With increasing true plastic strain, an increase in hardness can be achieved within the specimen, see **Figure 3 a**). For true plastic strains higher than  $\varphi = 0.1$ , the hardness values differ in the component areas. At a true plastic strain of  $\varphi = 0.7$ , the maximum hardness of 385 HV1 was determined in the centre area of the specimen (D) and the lowest hardness values of around 360 HV1 was measured in area (C).

**Figure 3** b) shows the dependence of the forming speed on the resulting hardness. The results refer to the sample area (D) at a forming temperature of  $T = 20\text{ }^{\circ}\text{C}$ . The hardness values were measured in specimens with the lower true plastic strains. At the low true plastic strains of  $\varphi = 0.1$  and  $\varphi = 0.3$ , no influence of the forming speed on the hardness could be determined. Here, hardness values of  $250 \pm 10$  HV1 for the true plastic strain of 0.1 and  $300 \pm 2$  HV1 for the true plastic strain  $\varphi = 0.3$  could be determined. An influence of the forming speed on the deformation-induced martensitic phase transformation could only be determined at a true plastic strain of 0.7. The lower the forming speed, the higher the hardness values. These results could also be attributed to the above-mentioned effect of adiabatic heating. The higher the forming temperature or the resulting component temperatures due to the dissipation heat, the more the deformation-induced martensitic phase transformation is reduced.

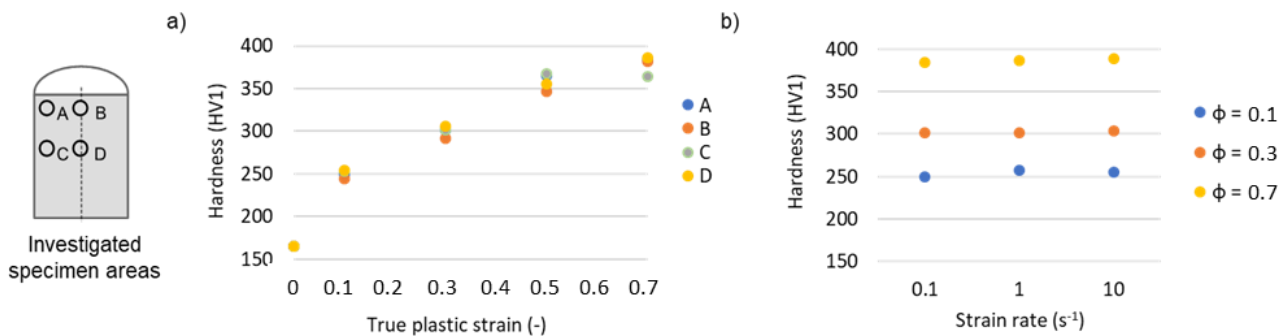


**Figure 3** Hardness of X5CrNi18-10 of different true plastic strains  $\varphi$  in different part areas (a) and hardness under different strain rates while forming (b)

The upsetting tests with true plastic strain of 0.7 are used to determine the flow curves of X5CrNi18-10 for the numerical process design at process-relevant temperatures between  $T = -15$  and  $300\text{ }^{\circ}\text{C}$  with constant strain rates of  $\dot{\varphi} = 0.1, 1$  and  $10\text{ s}^{-1}$ . **Figure 4** shows the flow curves for  $\dot{\varphi} = 0.1$  and  $10\text{ s}^{-1}$  determined as a function of forming temperature and speed. The flow curves show a strong temperature dependence since the flow stress of the material decreases with an increasing forming temperature. Furthermore, a small strain rate dependence can be seen in this temperature range. The flow stress increases slightly with increasing forming speed.

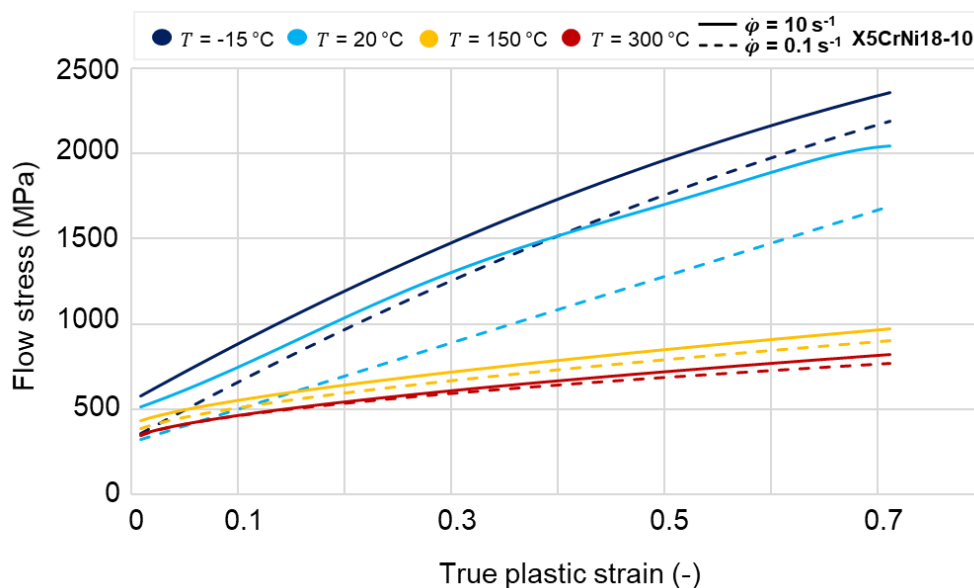


**Figure 4** Flow curves of X5CrNi18-10 with varied temperatures and forming speed

The influence of the set surface topologies in combination with the different lubricants on the contact conditions of the workpiece - tool system was characterized by means of ring upsetting tests on the Weingarten screw press, see **Table 1**. The following table summarizes the results of these investigations. The resulting surface topologies of the respective manufacturing processes are shown in **Table 1**. Three-dimensional optical surface measurements (Keyence VR 3200) were carried out to characterize the texturing intensities. In addition to the different surface topologies of the tools, different lubricants were also considered within the scope of these investigations. The lubricant used has a decisive influence on the tribological system between tool and workpiece thus on the friction between these components (e.g. displacement or lubrication pocket effect).

The lowest friction factor of 48 variants at  $T = 20\text{ °C}$  of  $m = 0.38$  was determined using  $\text{MoS}_2$  in combination with the blasted surface topology. The highest friction factor  $m = 1$  could be determined independently of the lubricant with the surface topology turning II. In this case the workpiece adheres to the tool during forming. In practice, this would lead to extreme tool wear and high tool loads. The next highest friction factor of  $m = 0.60$  was determined for the combination of molybdenum sulphide and the surface topology via grinding. These three friction factors are applied in the numerical process design in a friction factor model to portray the bandwidth of possible conditions. For all simulations, the initial workpiece and tool temperature of  $20\text{ °C}$  was used as flow behavior of X5CrNi18-10 in the temperature range down to  $-15\text{ °C}$  hardly differs.

**Table 1** Influence of surface topologies and lubricants on the friction factor at  $20\text{ °C}$

	Machining processes			
	Grinding	Blasting	Turning I	Turning II
Achievable average roughness $R_a$ ( $\mu\text{m}$ )	1.18	2.99	2.21	18.4
Max friction factor $m$	0.60 ( $\text{MoS}_2$ )	0.52 (Graphit)	0.58 ( $\text{MoS}_2$ )	1.00 ( $\text{MoS}_2$ , Teflon, Graphit)
Min. friction factor $m$	0.45 (Teflon)	0.38 ( $\text{MoS}_2$ )	0.43 (Teflon)	1.00 ( $\text{MoS}_2$ , Teflon, Graphit)

**Figure 5** shows the designed forming process (left) and the true plastic strain reached with different friction factors at  $T = 20\text{ °C}$  (right). Further, the figure shows the simulation results of the forming process taking into account the min./max. friction factors achieved depending on surface topology and lubricants. Furthermore, examples of rolling elements and their contact areas are shown.

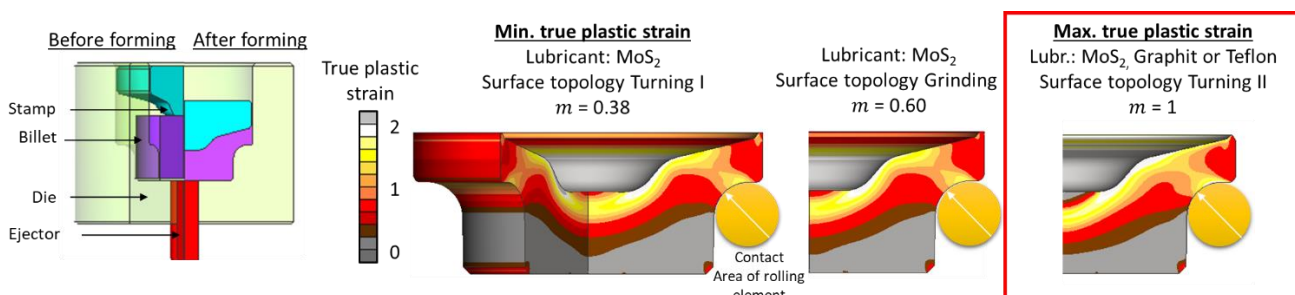


**Figure 5** Numerically investigated forming process under variation of lubricant and surface topology at a forming temperature of  $T = 20\text{ °C}$

Due to the designed forming process, the workpiece material is expanded and flows slightly over the die shoulder, which is reflected in inhomogeneous true plastic strains in the area of the running surface. The influence of the friction factors  $m = 0.39$  and  $0.6$  is low considering the individual boundary conditions via surface topology and the lubricant. The true plastic strain could only be further increased by means of deep turning grooves and high friction factors (Turning II), which would not be practicable in technical implementation

and lead to low tool service life. Nevertheless, the true plastic strain achieved in the area of the running surface of the angular ball bearing ring even exceeds the values previously determined in the upsetting tests. Therefore, it can be assumed that a higher strength is achieved in the forming process.

#### 4. CONCLUSION AND OUTLOOK

With the designed process, it is possible to produce the desired bearing inner ring preform by bulk forming. However, differences were determined with regard to the local true plastic strain. It is shown that the reached true plastic strain leads to high hardness and strength, since more martensite is generated. The forming process at lower temperatures should significantly increase the service life of the angular contact ball bearings made of stainless steel X5CrNi18-10.

Further, the preforms of the ball bearing inner rings will be produced by forming and afterwards machined to its final geometry. The service life of the components will then be investigated by a developed test stand. Furthermore, the influence of a higher degree of forming is to be investigated by using an extrusion process for component manufacture.

#### ACKNOWLEDGEMENTS

***The authors would like to thank the German Research Foundation (DFG) for the financial support of the project (Project-No. 423160066)***

#### REFERENCES

- [1] WULFSBERG, J.P., HINTZE, W., BEHRENS, B.A. *Production at the Leading Edge of Technology*. Berlin, Heidelberg: Springer Berlin / Heidelberg, 2019.
- [2] KNIGGE, J. *Lokale Martensitbildung in metastabilen austenitischen Stählen durch Verfahren der Massivumformung*. Hannover, 2015. Dissertation. Leibniz University Hannover.
- [3] BEHRENS, B.A., HÜBNER, S., BOUGUECHA, A., KNIGGE, J., WEILANDT, K. Local Strain Hardening of Metal Components by Means of Martensite Generation. *Advanced Materials Research*. 2010, vol. 137, pp. 1-33.
- [4] WEIßBACH, W., DAHMS, M., JAROSCHEK, C. *Werkstoffe und ihre Anwendungen*. Wiesbaden: Springer Fachmedien Wiesbaden, 2018.
- [5] BARGEL, H.-J., CARDINAL, P., HILBRANS, H., HÜBNER, K.-H., KRÜGER, O., SCHULZE, G. *Werkstoffkunde*. Berlin, Heidelberg: Springer Berlin Heidelberg, 2004.
- [6] OLSON, G.B., COHEN, M. Kinetics of strain-induced martensitic nucleation. *Metallurgical Transactions A*. 1975, vol. 6, no. 4, pp. 791-795.
- [7] BARENBROCK, D. *Influence of deformation-induced martensite transformation on the crack propagation behaviour of austenitic steels*. Hannover, 2002. Dissertation. Leibniz University Hannover.
- [8] LINDENBERG, H.U., KAZMIERSKI, O., OTTO, A. Kaltgewalztes Band aus nichtrostenden Edelstählen und die Anwendungspotentiale. *Stahl und Eisen*. 2000, vol. 120, no. 5, pp. 37-42.